ELECTROCHEMICAL STUDIES ON 1-AZOPHENYLAZULENE

Eleonora-Mihaela UNGUREANU[1], Alexandru C. RĂZUŞ[2], Liviu BÎRZAN[3], Mariana-Ştefania CREŢU[4], Elena Diana GIOL[5]

S-a realizat un studiu electrochimic pentru 1-azofenilazulena (A) în soluţii de acetonitril prin voltametrie ciclică (CV), voltametrie puls-diferenţială şi electrod disc-rotitor. S-a studiat formarea de filme de poli(A). Electrozii modificaţi cu filme de poli(A) au fost caracterizaţi prin CV în soluţii de electrolit suport şi în soluţii de ferocen în electrolitul suport.

The electrochemical study of 1-azophenylazulene (A) in acetonitrile solutions was performed by cyclic voltammetry (CV), differential pulse voltammetry and rotating disk electrode. The poly(A) film formation was studied. The poly(A) modified electrodes were characterised by CV in solutions of supporting electrolyte and in ferrocene solutions in the supporting electrolyte.

Keywords: 1-azophenylazulene, cyclic voltammetry, differential pulse voltammetry, rotating disc electrode, film formation.

1. Introduction

The study of the electrochemical behaviour of the azoazulene derivatives is important in connection with these compounds applications as molecular switches, for NLO, or electrochromic materials, as well as, for the modification of electrode properties [1, 2]. The research of the electrochemical properties is an essential step in the evaluation of these compounds reactivity both in the electrochemical and chemical reactions. Among the reactions of major interest from synthetic point of view, the electrochemical halogenation presents a special interest due to the synthetic potential of the halogen derivatives which can be

[1] Prof., Department of Applied Chemistry and Electrochemistry, Faculty of Applied Chemistry and Materials Science, University POLITEHNICA of Bucharest, Romania, em_ungureanu2000@yahoo.com
[2] Senior Researcher, Institute of Organic Chemistry "C. D. Nenițescu", of the Romanian Academy, Bucharest, Romania
[3] Researcher, Institute of Organic Chemistry "C. D. Nenițescu", of the Romanian Academy, Bucharest, Romania
[4] PhD student, Department of Applied Chemistry and Electrochemistry, Faculty of Applied Chemistry and Materials Science, University POLITEHNICA of Bucharest, Romania
[5] Student, Department of Applied Chemistry and Electrochemistry, Faculty of Applied Chemistry and Materials Science, University POLITEHNICA of Bucharest, Romania

relatively easily transformed in other compounds. The study of electrochemical halogenation of certain azulenes and the characterization of electrohalogenation products constituted the topic of previous works, in which the electrohalogenation mechanism and preparation of corresponding halogen derivatives were described [3, 4]. The synthesis of azulene halogen derivatives is important as well from practical point of view, these compounds having potential properties specific to nonlinear optics [5]. Being a polar group (the dipole moment of azulene is μ=1 Debye), azulene moiety can be a good precursor for push-pull molecules [6, 7]. Another electrochemical reaction of major interest for the azulene compounds is the film formation through electropolymerization in order to obtain modified electrodes [8].

This paper is a part of the studies devoted to the examination of the electrochemical properties of azulene derivatives which was performed in order to establish correlations between the structure and the properties of a large range of azulene compounds [9]. The title compound, 1-azophenylazulene (**A**), can be considered as a parent compound, because by substituting the azulene or phenyl moiety a large variety of structures can be generated, leading thus, to compounds with quite various properties. This justifies the interest for thoroughly studying its electrochemical properties and for the formation of azulene films by electropolymerization.

2. Experimental

Acetonitrile, CH_3CN (Rathburn, HPLC grade), tetra-*n*-butylammonium fluoroborate ($TBABF_4$) and tetra-*n*-butylammonium perchlorate (TBAP) from Fluka were used as received, as solvent and supporting electrolytes, respectively. 1-azophenylazulene (**A**) has been obtained by specific chemical reactions of azulenes [9]. Its structure and characteristics have been confirmed by elemental and spectral (^{1}H-RMN, ^{13}C-RMN, GC-MS) analyses.

Cyclic voltammetry (CV), differential pulse voltammetry (DPV) and rotating disk electrode (RDE) electrochemical experiments were conducted in a conventional three-electrode cell under argon atmosphere at 20^{o}C using a PGSTAT 12 AUTOLAB potentiostat. The working electrode was a glassy carbon (GC) disk (3 mm in diameter) polished with 200 μm diamond paste. The Ag/10mM $AgNO_3$ in CH_3CN + 0.1M $TBABF_4$ system was used as reference electrode. A platinum wire immersed in CH_3CN + 0.1M $TBABF_4$ system was used as counter electrode. All potentials were referred to the potential of ferrocene/ferricinium (Fc/Fc^+) couple, which in our experimental conditions was 0.07 V.

CV experiments have been performed at a scan rate of 0.1 V/s and at different scan rates (0.1 ÷ 10V/s) when the influence of the scan rate was

investigated. DPV curves have been recorded at 10mV/s with a pulse height of 25mV and a step time of 0.2s. RDE investigations have been usually performed at a scan rate of 5mV/s and at different rotations rates (500 ÷ 3000rpm). All electrochemical investigations have been done in CH_3CN + 0.1 M $TBABF_4$ as supporting electrolyte.

The films have been synthesized in millimolar solutions of **A** in CH_3CN + 0.1M TBAP, by cycling the potential or by controlled potential electrolysis (CPE). The polymerization charge in CPE has been calculated by integration of the current in time. The modified electrodes (GC|poly**A**) have been tested by CV (at a scan rate of 0.1 V/s) in two electrolytes: **i)** CH_3CN + 0.1 M TBAP, in the domain of their electroactivity, and **ii)** 0.5 mM ferrocene in CH_3CN + 0.1 M TBAP in the domain of ferrocene activity.

3. Results and Discussion

DPV, CV, and RDE experiments have been performed in millimolar solutions of 1-azophenylazulene (**A**) in acetonitrile solutions. The anodic and cathodic curves for the supporting electrolyte (0.1 M $TBABF_4$, CH_3CN) were also recorded and they are shown with dotted lines in all figures.

3.1. DPV study

Fig. 1 shows the DPV curves obtained in solutions of 1-azophenylazulene at different concentrations (0.5 – 3 mM) in 0.1 M $TBABF_4$, CH_3CN. Anodic and cathodic curves are represented on the graph. In the anodic region of these DPV curves there are 4 peaks representing 4 main anodic processes **1a - 4a**. **1a** and **2a** could be attributed to the substrate oxidation, **3a** is due to the background oxidation and **4a** is uncertain as it is overlapped on the supporting electrolyte oxidation. In the cathodic region 4 reduction processes of **A** are noticed, **1c - 4c**. Linear dependences of the peak currents and potentials on concentration can be seen inserted in the Fig 1c and Fig.1b, respectively, and their characteristics are given in Tables 1 and 2.

Table 1

Influence of concentration X(mM) on peak potentials Y(V) from DPV data (Fig. 1b)

Anodic Peaks	Equation X(mM); Y(V)	Cathodic Peaks	Equation X(mM); Y(V)
1a	Y = 0.527 + 0.006 X	1c	Y = - 1.675 - 6.7E-4 X
2a	Y = 0.867 + 0.034 X	2c	Y = - 2.275 + 0.097 X
3a	Y = 1.177 + 0.007 X	3c	Y = - 2.135 - 0.003 X
4a	Y = 1.921 + 0.012 X	4c	Y = - 2.358 - 0.006 X

Table 2

Influence of concentration X(mM) on peak currents Y(A) from DPV data (Fig. 1c)

Anodic Peaks	Equation X(mM); Y(A)	Cathodic Peaks	Equation X(mM); Y(A)
1a	Y = 2.523E-6 + 6.358E-6 X	1c	**Y = - 3.167E-6 - 8.263E-6 X**
2a	Y = 4.479E-6 + 5.972E-6 X	2c	Y = - 5.04E-6 - 2.535E-6 X
3a	Y = 9.323E-6 + 0.9169E-6 X	3c	Y = - 3.776E-6 - 3.717E-6 X
4a	Y = 15.19E-6 + 0.7321E-6 X	4c	Y = - 0.9264E-6 - 4.031E-6 X

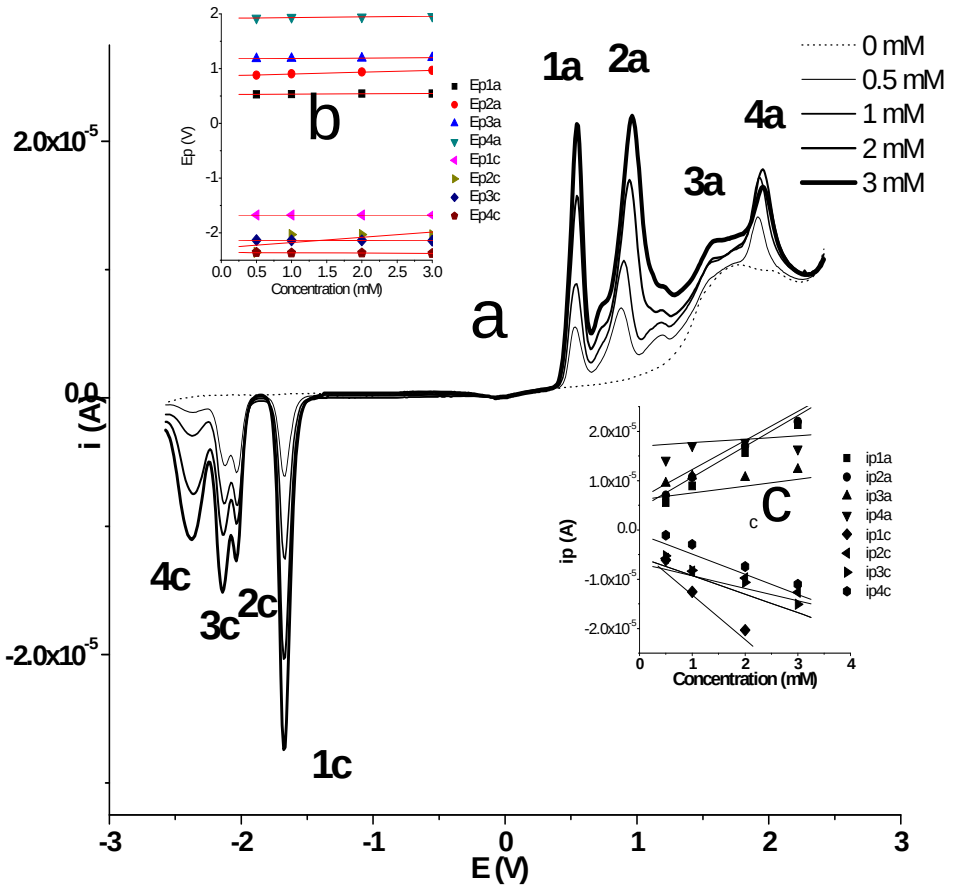

Fig. 1 (a) Anodic and cathodic DPV curves at different concentrations of **A** in 0.1M $TBABF_4$, CH_3CN; glassy carbon (3mm in diameter); (b) Dependence of the peak potential on the concentration; (c) Dependence of the peak currents on the concentration

As it can be seen from Table 1, the potentials of the first peaks of oxidation (**1a**) and reduction (**1c**) are not influenced by **A** concentration. As opposed to these, the peaks corresponding to the second electron transfers (anodic or cathodic) have potentials which are influenced by substrate concentration (having slopes of 34 and 97 mV/mM for **2a** and **2c**, respectively). The anodic peak potentials (E3a, E4a) are slightly dependent on substrate concentration (slopes of about 10 mV/decade), as well as the cathodic peak potentials (E3c – E4c). This behaviour is in agreement with an ECE mechanism of electro oxidation and reduction of **A** for the peaks **1a**, **2a**, and **1c**, **2c**. The peaks **1a** and **1c** correspond to the formation of the radical anion and radical cation of **A**, respectively. These electron transfers are followed by stabilization reactions and other electron transfers (**2a** and **2c**, **3c**, **4c**). The equations of the linear dependences of the **peak currents** on concentration are seen in Table 2. For **1a** and **2a** there is a linear dependence of the peak currents on concentration with similar slopes (~ 6 μA/mM), while for **3a** and **4a**, the slopes are about 6 times smaller (~ 1μA/mM). This is a proof that **3a** and **4a** processes are mainly due to the background oxidation. The slope (in absolute value) for **1c** is a little higher than for **1a.** For **2c** – **4c** processes the slopes are about half of the slope for **1c**. This result can be interpreted as followed: after the first electron gain, with the formation of an anion radical, a splitting of this in 3 fragments (which can be reduced further with similar rates) occurs. So, **2c**, **3c**, and **4c** are successive electron gains of each fragment of the molecular fragments. The linear dependence of DPV peaks on concentration shows that the DPV curves could be used in analytical determinations of the substrate **A** by this electrochemical method.

3.2. CV study

Fig. 2a gives the CV anodic and cathodic curves at different concentrations (0 – 3 mM) of **A** in 0.1 M $TBABF_4$, CH_3CN. The CV curves allowed putting in evidence the same processes (**1a - 4a**, and **1c** – **4c**), which were shown by DPV. In Fig. 2b and 2c are given the dependences of the peak potentials and currents on concentration, respectively. The CV peak potentials are little influenced by concentration (Table 3). The CV peak currents are linearly dependent on concentration with different slopes: **1a** and **1c** have about the same slope (in absolute value) of 9 μA/mM. A comparison of the slope (S) absolute values shows that: $S_{1a} < S_{2a} < S_{3a} < S_{4a}$; $S_{1c} \sim S_{2c} \sim S_{4c;}$ $S_{3c} > S_{1c}$. We got linear dependences on concentration for all peaks in CV.

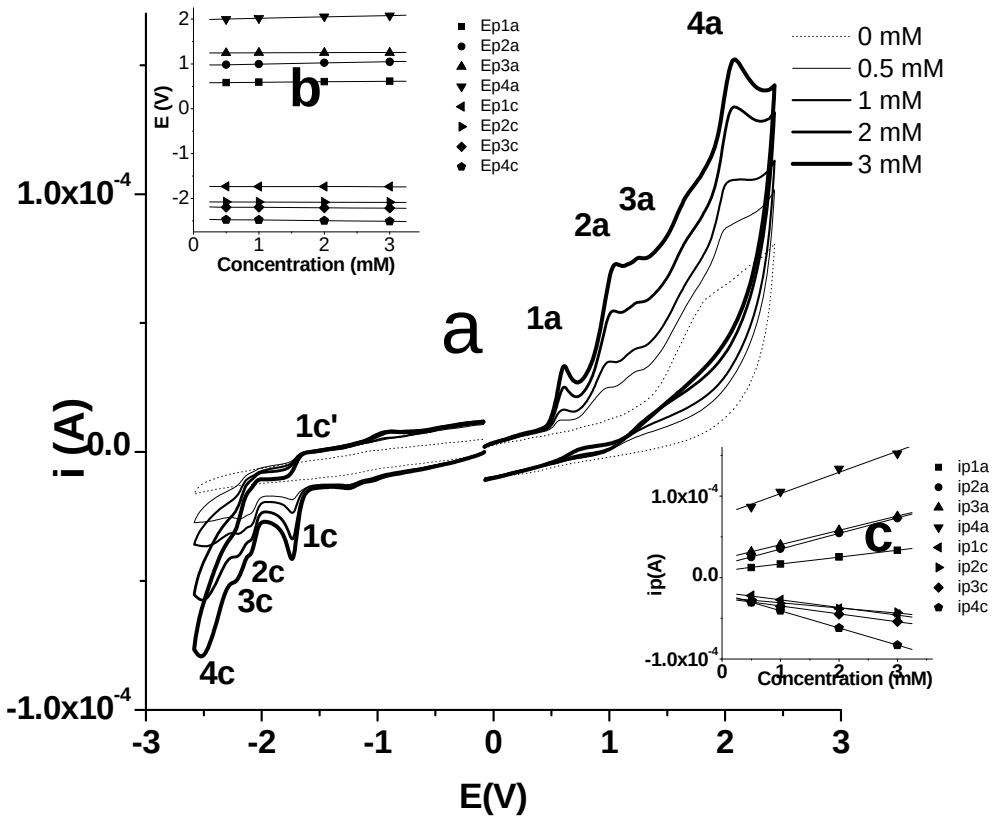

Fig 2. (a) Anodic and cathodic CV curves on glassy carbon (3mm in diameter) at different concentrations of **A**; 0.1M $TBABF_4$, CH_3CN; (b) Dependence of the peak potential on the concentration; (c) Dependence of the peak currents on the concentration

Fig. 3 shows the influences of the scan range and scan rate on the CV curves obtained in a solution (3mM) of **A**. Fig. 3a shows the anodic and cathodic CV curves on increasing domains of scanning. The obtained curves enabled to evidence that all anodic processes are irreversible in the investigated range of scan rates (< 10V/s), while the cathodic peak **1c** is quasi-reversible, having a counter peak in the return scan **1c'**. The other cathodic peaks are also quasi-reversible, having small counter peaks in the reverse scans.

Table 3

Influence of concentration X(mM) on peak potentials Y(V); data from Fig. 2b

Anodic Peaks	Equation X(mM); Y(V)	Cathodic Peaks	Equation X(mM); Y(V)
1a	Y = 0.579 + 0.011 X	1c	Y = -1.736 - 0.002 X
2a	Y = 0.968 + 0.027 X	2c	Y = -2.081 - 0.003 X
3a	Y = 1.244 + 0.003 X	3c	Y = -2.191 - 0.009 X
4a	Y = 1.983 + 0.033 X	4c	Y = -2.468 - 0.015 X

Table 4

Influence of concentration X(mM) on peak currents Y(A); data from Fig. 2c

Anodic Peaks	Equation X(mM); Y (A)	Cathodic Peaks	Equation X(mM); Y (A)
1a	Y = 8.168E-6 + 8.492E-6 X	1c	Y = -1.789E-5 - 9.398E-6 X
2a	Y = 1.588E-5 + 1.915E-5 X	2c	Y = -2.455E-5 - 6.365E-6 X
3a	Y = 2.292E-5 + 1.753E-5 X	3c	Y = -2.522E-5 - 9.656E-6 X
4a	Y = 7.701E-5 + 2.610E-5 X	4c	Y = -1.970E-5 - 2.106E-5 X

Table 5

Influence of the logarithm of the scan rate X (V/s) on peak potentials Y (V); data from Fig. 2b

Anodic Peaks	Equation X(log(V/s)); Y(V)	Cathodic Peaks	Equation X(log(V/s)); Y(V)
1a	Y = 0.699 + 0.099 X	1c	Y = -1.812 - 0.079 X
2a	Y = 1.149 + 0.156 X	2c	Y = -2.151 - 0.071 X
3a	Y = 1.449 + 0.222 X	3c	Y = -2.287 - 0.099 X
4a	Y = 2.334 + 0.274 X	4c	Y = -2.602 - 0.082 X

Table 6

Influence of square root of the scan rate X (V/s) on peak currents Y (A); data from Fig. 2c

Anodic Peaks	Equation X(sqrt(V/s));Y(A)	Cathodic Peaks	Equation X(sqrt(V/s));Y(A)
1a	Y = -2.521E-5 + 1.557E-4 X	1c	Y = -1.829E-5 - 9.838E-5 X
2a	Y = -4.660E-5 + 3.106E-4 X	2c	Y = -3.610E-6 - 1.189E-4 X
3a	Y = -9.872E-5 + 4.349E-4 X	3c	Y = -1.316E-5 - 1.298E-4 X
4a	Y = -4.335E-5 + 6.168E-4 X	4c	Y = -2.710E-5 - 1.756E-4 X

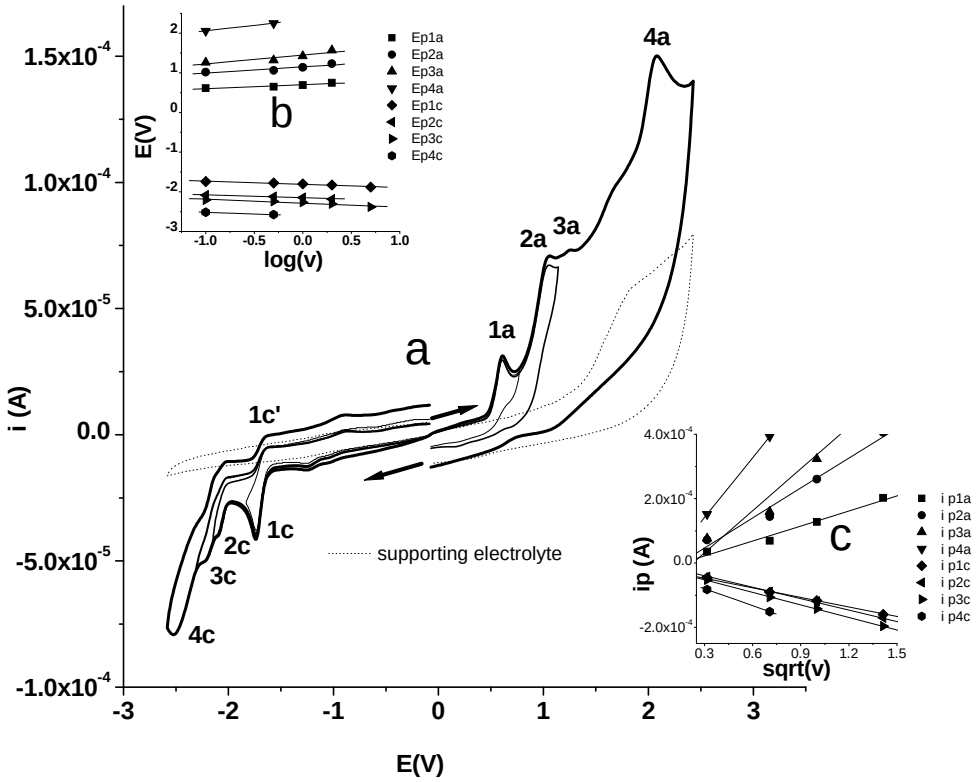

Fig. 3. (a) Anodic and cathodic CV curves on different domains at the concentration of 3mM **A** in 0.1M $TBABF_4$, CH_3CN; glassy carbon (3 mm in diameter); (b) Dependence of the peak potential on the logarithm of the scan rate; (c) Dependence of the peak currents on the square root of the scan rate

The dependences of the CV peak currents on the square root of the scan rate (shown in Fig. 3c) are linear and their equations are given in Table 6. The anodic peaks **1a** and **2a** have different slopes when the scan rate varies (155 and 310 μA $V^{-1/2}$ $s^{1/2}$, respectively). The peaks for the overlapped processes (**3a**, **4a**) have bigger slopes (over 400 μA $V^{-1/2}$ $s^{1/2}$). The cathodic peaks **1c** - **3c** have similar slopes (between 100 and 130 μA $V^{-1/2}$ $s^{1/2}$), while **4c** has a slope of about 180 (μA $V^{-1/2}$ $s^{1/2}$). This difference in the behaviour of anodic and cathodic peaks obtained by CV, is in agreement with the behaviour observed in DPV, and is the result of different mechanisms of oxidation and reduction.

Successive CV scans in the anodic range (Fig. 4) show a continuous decrease of the peak currents in successive cycles and the appearance of a new couple having a pair of peaks (**0a** and **0a'**) at the expense of the peak **1a**. The couple **0a**/**0a'** appears at potentials less positive than **1a** and corresponds to the

oxidation of the poly**A** film on the electrode surface (polyA is oxidized at lower potentials than the starting monomer). Its formation will be shown further in detail.

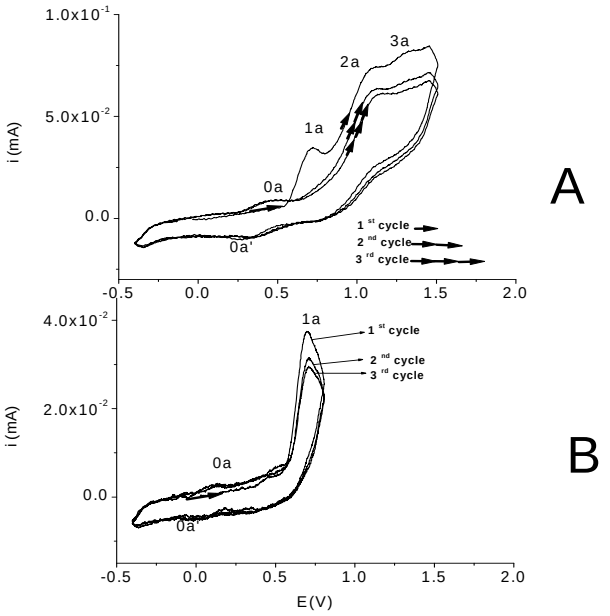

Fig. 4. Successive CV anodic curves (0.1 V/s) on glassy carbon (3 mm in diameter) in **A** solution (1mM) in 0.1 M $TBABF_4$, CH_3CN on different scan ranges

3.3. RDE study

Fig. 5 presents the anodic and cathodic RDE curves obtained at different rotation rates. From the RDE currents there can be seen that the numbers of electrons implied in the first anodic (**1a**)4 and cathodic (**1c**) processes are similar. In consequence, the intermediates in these anodic and cathodic processes are formed by one-electron transfer, being the anion radical or the cation radical, respectively. The evaluation of the number of electrons in the other cathodic processes (**2c - 4c**) is difficult to be discussed because they appear overlapped.

Examining the RDE shapes of the curves from Fig. 5 obtained in the anodic and cathodic scans, there can be seen that they are very different. In the cathodic scans the limiting currents are normally increasing with the rotation rate. However, the successive cathodic processes are difficult to be separated. The separation is evident only for the processes **1c** and **2c**. The reason for this behaviour is that the other processes (**2c - 4c**) are too close to be seen as distinct waves. In the anodic scans the currents are increasing with the rotation rate only at the beginning of the process **1a**. The process **2a** cannot be seen on RDE. The intermediate formed in **1a**, normally assumed to be the cation radical, seems to be

very reactive. The sudden decrease of the current after the first oxidation process indicates the covering of the electrode surface with a film. That is why the aspect of the RDE anodic curve is like a *peak* instead of having an S shape. As the rotation rates increase, the anodic RDE-*peak* currents increase too. However, the width of the RDE-*peak* is smaller, as expected if we assume a polymerization process (Fig. 6a). At small concentration (0.5 mM) the two processes **1a** and **2a** can be seen distinctly, but only at a small rotation rate (500 rpm), as shown in Fig. 5a. In this case, the process **1a** has limiting currents which normally increase linearly with the square root of the rotation rate (Fig 6b).

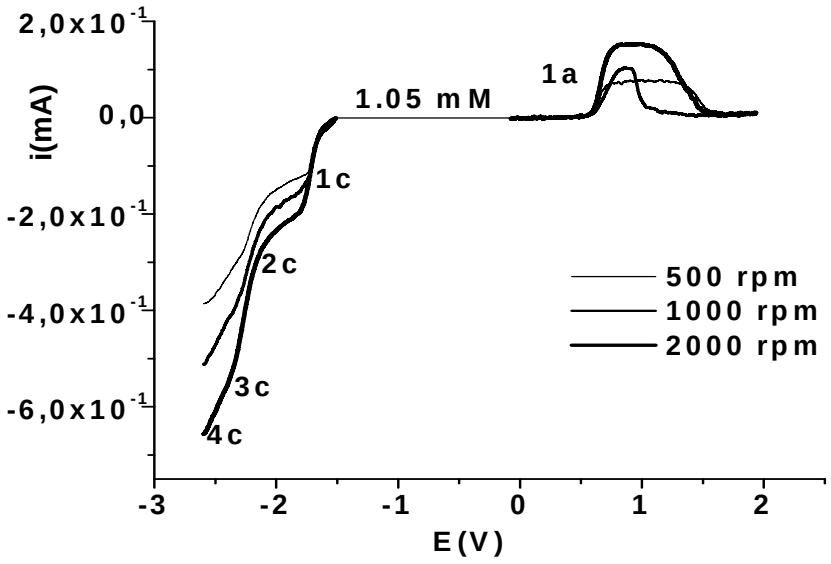

Fig. 5. Influence of rotation rate (rpm) on anodic and cathodic domains on glassy carbon (3 mm in diameter); 10mV/s; [**A**] = 1mM ; 0.1M $TBABF_4$, CH_3CN

Unusual shapes of the RDE curves have been found in the anodic range for different concentrations of the substrate **A** (Fig 6). As the concentration increases, the height of the RDE-*peak* increases, while its width decreases. The two anodic processes **1a** and **2a** are no more separated at higher rotation rates (1000 rpm). This confirms that a fast polymerization occurs during the process **1a**.

Fig 8 presents the RDE and CV anodic curves for two concentrations of **A** and at different scan ranges. All anodic processes can be seen only by CV in the larger domain of scanning (Fig. 8a), while the RDE curve has only a *peak* in the range of the process **1a**. In a shorter domain (Fig. 8b) the CV has the shape of an irreversible curve, and the RDE has the shape of a *peak*. These shapes are in agreement with the formation of a film on the electrode.

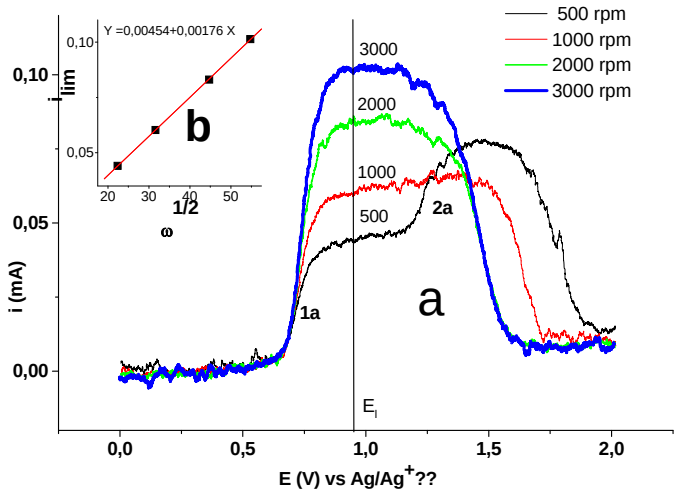

Fig 6. (a) Influence of the rotation rate on the RDE curves in anodic domain on glassy carbon (3mm in diameter) at different rotation rates*;* [**A]** = 0.5mM in 0.1 M $TBABF_4$, CH_3CN**;** (b) Linear dependence of limiting current of 1a process on the square root of the rotation rate ω (rpm)

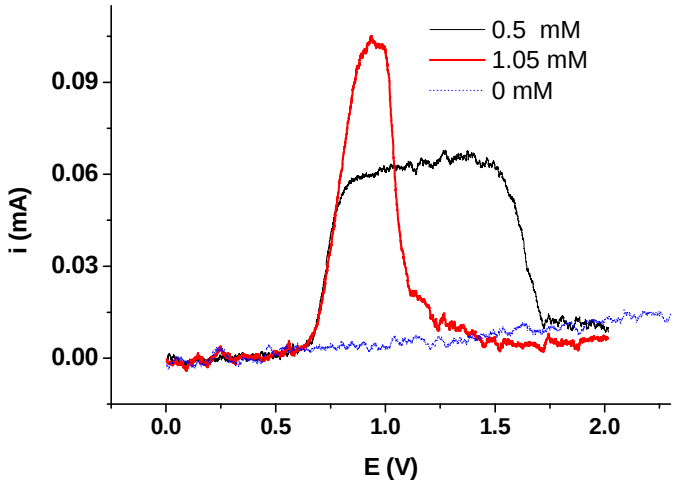

Fig. 7. Influence of **A** concentration in 0.1 M $TBABF_4$, CH_3CN solution on the RDE anodic curves; glassy carbon (3mm in diameter); 1000rpm; 5mV/s

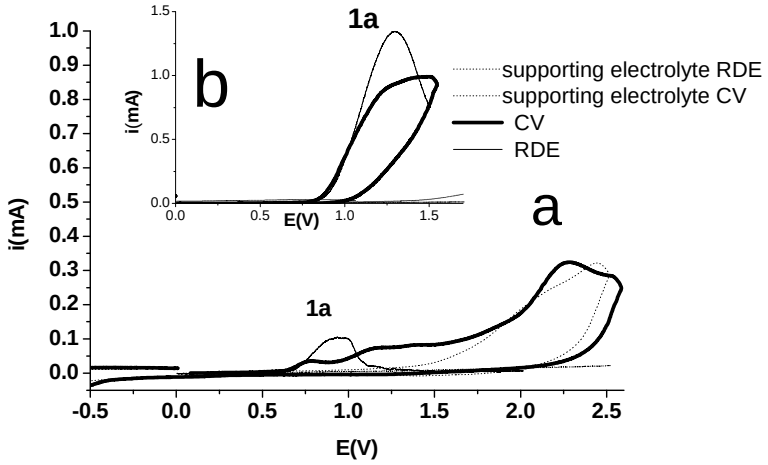

Fig. 8. RDE and CV (0.1V/s) anodic curves on glassy carbon (3mm in diameter) in 0.2mM (a) and 1mM (b) azoazulene solutions on different scan ranges

3.4. Film formation study

The film formation was first tried in CH_3CN + 0.1 M $TBABF_4$ as supporting electrolyte, but non-conductive films were obtained. Then the film formation was experienced in CH_3CN + 0.1 M TBAP system. As a result of the anodic polymerization in the domain of the first anodic process (**1a**), conductive polymeric films of **A** have been formed leading to a GC|poly**A** modified electrode. The electropolymerization of A was readily achieved in acetonitrile electrolyte. The monomer displays an irreversible oxidation peak around 0.7 V. PolyA films could be grown onto carbon disk electrode surfaces from 10mM in CH3CN 0.1M TBAP upon repeated scans in the -0.4 V to 0.6 V potential range (Fig. 9a). Formation of a conducting polyazulene film was evidenced by the growth of a quasi-reversible redox peak system centered around 0.25 V.

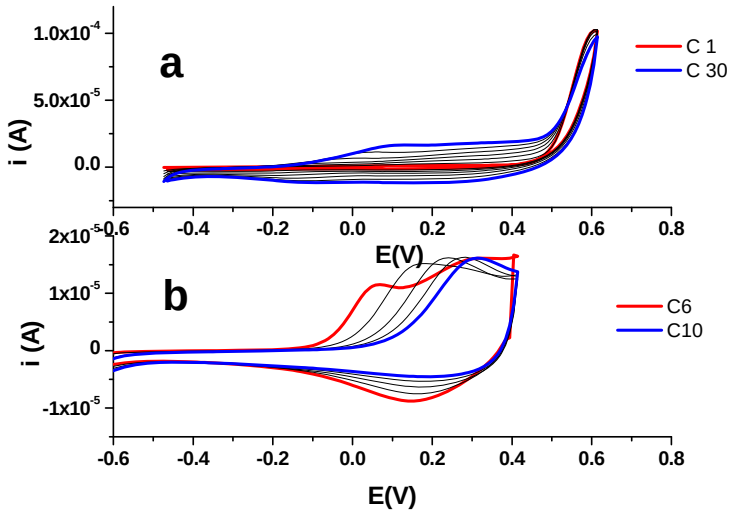

Fig. 9. Poly**A** film formation (a) in synthesis solution on glassy carbon electrode (3mm in diameter) by scanning in 30 successive cycles (each 5th cycle is shown between C1 and C30) and characterization (b) of the obtained modified electrode in the 5th and 10th CV cycles in transfer solution; 0.1V/s; 10mM A, 0.1M TBAP, CH_3CN

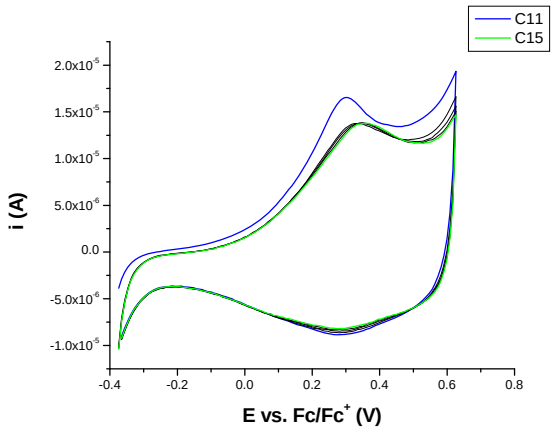

Fig. 10. Successive CV curves of the modified electrode in transfer solution (0.1 v/s)

Upon transfer into clean acetonitrile 0.1M TBAP electrolyte, the resulting C/polyA modified electrode retains this electroactivity (Fig. 9b). The CV for the modified electrode changes in the transfer solution, as it can be seen in Fig. 9b, the oxidation and reduction currents increase and the peak potentials shift to more positive values. A possible explanation for this change could be due to either i)

the presence of residual monomer in the porous layer film deposited on the electrode surface, which continues the polymerization when the electrode is scanned, or ii) the rearrangement of the film structure during the cycling in the supporting electrolyte.

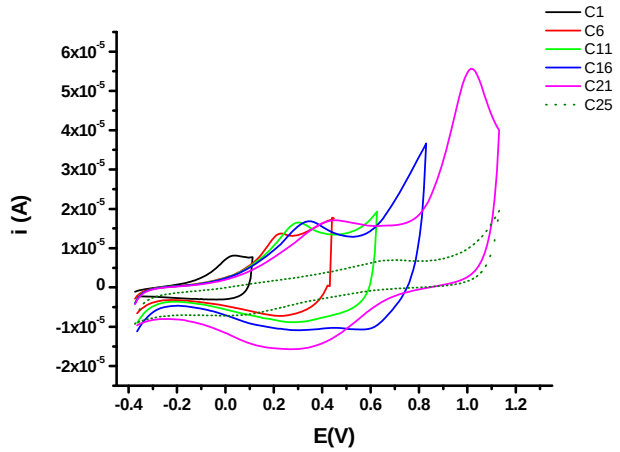

Fig. 11. CV (0.1V/s) curves of the poly**A** modified electrode (obtained by scanning) in transfer solution with increasing anodic limits of the scans; first cycle of each set of five is shown

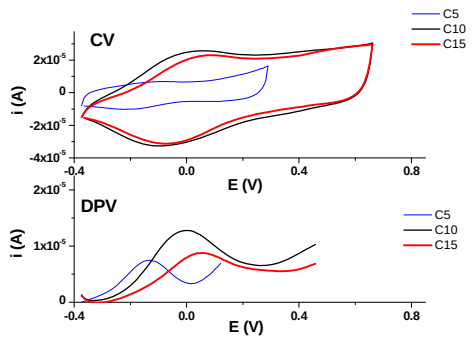

Fig. 12. CV and DPV curves of the modified electrode obtained by CPE (0.61V, 10mC) after 5; 10; 15 cycles in the transfer solution

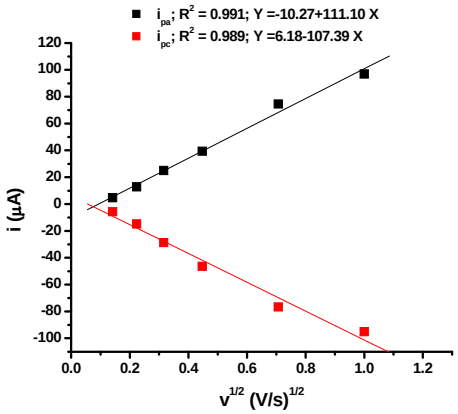

Fig. 13. Dependence of the peak currents for the modified polyA electrode obtained by CPE (0.61V, 10mC) in transfer solution upon the scan rate

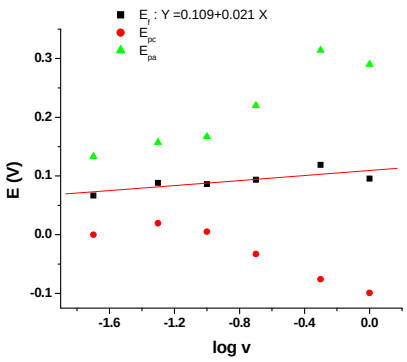

Fig. 14. Dependence of the peak potentials for the modified polyA electrode obtained by CPE (0.61V, 10mC) in transfer solution upon the scan rate

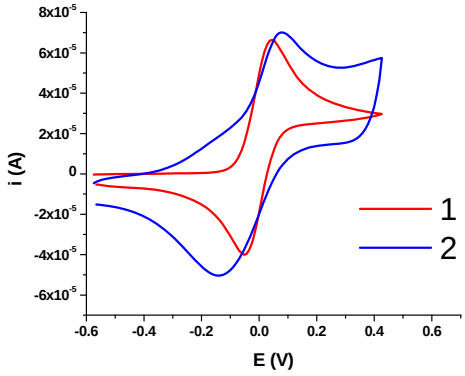

Fig. 15. CV of the bare (1) and modified (2) electrode in ferrocene solutions (1mM) in 0.1M TBAP, CH_3CN

Stable polymeric conductive films were obtained as shown in Fig 10, The modified electrodes with films of poly**A** were obtained either by scanning or by controlled potential electrolysis (CPE). Fig 10 presents 5 successive CVs of the GC|poly**A** modified electrode in the transfer solution (0.1 M TBAP, CH_3CN), showing the same currents in successive cycles. By scanning over 0.6 V (as seen in Figs. 10 and 11) the reversibility is lost and the film is overoxidized leading to an insulating film.

PolyA films could also be grown by controlled potential oxidation between 0.4 and 0.7V, i.e., at the threshold of the azulene oxidation wave. Typically, blue films with were obtained in CH3CN using polymerization charges over 1mC. These films are also modified in transfer solution during the scanning, as it was shown previously, as it can be seen from both CV and DPV curves (Fig. 12). Fig. 13 and 14 show linear dependences for the anodic and cathodic peak currents and potentials, respectively, of the modified polyA electrode in transfer solution upon the square root and the logarithm, respectively, of the scan rate.

The film formation was also proved by the different signals for ferrocene couple obtained on bare and polyA modified electrode (Fig. 15). The peak potentials are shifted and the difference between the peak potentials is much increased for the modified electrode.

4. Conclusions

The study performed by different electrochemical methods (DPV, CV, and RDE) enabled the assessment of the redox activity of 1-azo-phenyl-azulene.

The DPV curves gave the best evaluation of the peak potentials, as well as the actual number of redox processes. This method distinctly provides the processes that occur at quite close potentials, which appear as separate peaks, and is the best analytical method among the ones investigated in this study.

The CV curves enabled to establish the reversible or irreversible character of each electrochemical process, and to put in evidence the film formation by scanning in the anodic range.

The RDE curves enabled the estimation of the relative number of electrons implied in the main electrochemical processes (the formation of the cathion radical and of the anion radical), and proved also the film formation.

The methods used in this paper gave complementary knowledge about the electrochemical behaviour of 1-azo-phenyl-azulene, as well as about the film formation. Even if the poly**A** films are susceptible to overoxidation, the variation of the potential and charge enabled the preparation of stable polyazoazulene films.

Acknowledgments

Financial support from CNMP 71-067 REMORESE and 87/2006 CNCSIS contracts is gratefully acknowledged.

R E F E R E N C E S

[1] *G. Iftime, P. G. Lacroix, K. Nakatani, A. C. Răzuş,* Tetrahedron Lett., **39** (1998) 6853-6856.
[2] *P. G. Lacroix, I.. Malfant, G. Iftime, A. C. Răzuş, K. Nakatani, J. A. Delaire*, Chem. Eur. J., **6** (2000) 2599-2608.
[3] *E.-M. Ungureanu, A. C. Răzuş, L. Bîrzan, G. Buică, M. Creţu, C. Enache*, Elchim. Acta, **52** (2006) 794-803.
[4] *E.-M. Ungureanu, A. C. Răzuş, L. Bîrzan, George Buică, M. Creţu*, University POLITEHNICA of Bucharest SCIENTIFIC BULLETIN, **67** (2005), 3, 81-88.
[5] *O. Fernandez, P. Marquez, J. Marquez, W. Velasquez,* Rev. Tec. Ing. Univ. Zulia, **25**, 2002, 127.
[6] *G. W. Wheland, D. E. Mann* J. Chem. Phys. **17** (1949) 264.
[7] *A. G. Anderson, B. M. Steckler* J. Am. Chem. Soc. **81** (1959) 4941-4946.
[8] *S. Bargon,* IBM J. Res. Develop. **27**, 4, July 1983, 330-341.
[9] *E.-M. Ungureanu, A. C. Răzuş, L. Bîrzan, M.-S. Creţu, G.-O. Buică*, Electrochimica Acta **53** (2008) 7089-7099.
[10] *A. C. Răzuş, L. Bîrzan, S. Nae, C. Niţu, V. Câmpeanu,* Rev. Chim. (Bucharest) **52** (2001) 188-192.